J. Phys. Chem. A **1998,** *102,* 7143−7148

Bond Dissociation Energies and Heats of Formation for Fluorinated Ethers: E143A (CH_3OCF_3), E134 (CHF_2OCHF_2), and E125 (CF_3OCHF_2)

D. A. Good and J. S. Francisco*

Department of Chemistry and Department of Earth and Atmospheric Sciences, Purdue University, West Lafayette, Indiana 47907-1393

Received: March 13, 1998; In Final Form: June 2, 1998

Using G2 and G2(MP2) ab initio methodology, we have investigated the thermodynamics of the fluorinated ethers CH_3OCF_3 (E143a), CHF_2OCHF_2 (E134), and CF_3OCHF_2 (E125) and their corresponding ether radicals. The heats of formation (ΔH_f) of each fluorinated ether and radical at 298 K are −212.7 kcal mol^{-1} for E143a, −259.1 kcal mol^{-1} for E134, −314.5 kcal mol^{-1} for E125, −163.2 kcal mol^{-1} for CH_2OCF_3, −205.1 kcal mol^{-1} for CF_2OCHF_2, and −261.0 kcal mol^{-1} for CF_2OCF_3. In addition, we have determined the CH bond dissociation energy of each ether and compared it with literature values.

I. Introduction

Partially fluorinated ethers, E143a (CH_3OCF_3), E134 (CHF_2OCHF_2), and E125 (CF_3OCHF_2), have been proposed as potential chlorofluorocarbon replacements because of their lack of chlorine and their resulting low ozone depletion potentials. They are also favored because of their suspected short atmospheric lifetimes compared with analogous hydrofluorocarbons (HFCs).[1,2] Once released into the atmosphere, degradation of the ether is initiated by tropospheric hydroxyl radicals ($^\bullet$OH) to produce water and an ether radical, as shown in reaction 1

$$CH_3OCF_3 + {}^\bullet OH \rightarrow {}^\bullet CH_2OCF_3 + H_2O \qquad (1)$$

The rate of this first step determines the atmospheric lifetime of the ether, which in turn is used to estimate the potential of the ether to perturb global climate and interact with the ozone layer of the stratosphere.

In contrast to the studies of Zhang et al.[1] and Cooper et al.,[2] the work of Hsu et al.[3] has indicated significantly slower reaction rates for the hydroxyl radical reacting with both CHF_2OCHF_2 and CF_3OCHF_2, which translates into significantly longer atmospheric lifetimes than previously estimated. Longer atmospheric lifetimes would increase the potential for interaction between the ozone layer and the degradation products of ethers if reactions from formed degradation products could affect ozone. Knowledge of how these species interact in the Earth's atmosphere will be necessary to determine the full impact that these ethers have on the environment. The thermodynamic stability of the ether and ether radical product from reaction 1 will be useful for such an analysis, but the relative stability of each ether and its corresponding thermodynamics have yet to be determined. Heats of formation for these ether species can be used to ascertain the feasibility of potential atmospheric degradation pathways. This work determines, using high accuracy ab initio methodology, the heats of formation of E143a, E134, E125, and each corresponding radical. This information is important and valuable in assessing potential chemistry involving fluorinated ethers.

II. Methodology

All calculations were performed with the Gaussian 94 package of programs.[4] Geometry optimizations were carried out for all structures to >0.001 Å for bond lengths and 0.1° for angles. Using these geometries, a frequency calculation was performed at the second-order Moller-Plessset (MP2) level with restricted wave functions for closed shell, and unrestricted for open-shell systems, with all orbitals active. These optimizations were carried out with the medium split valence set, 6-31G(d), which includes polarization functions on heavy atoms. Optimizations were also performed with the Becke nonlocal three-parameter exchange and correlation functional with the Lee−Yang−Parr correctional functional method (B3LYP).[5] The B3LYP calculations were performed with the large 6-311++G(3df,3pd) basis set. The G2 and G2(MP2) energies were calculated using G2 methodology.[6−8] From a set of 125 test cases, there exists an average absolute deviation of 1.21 kcal mol^{-1} between G2 and experiment, whereas G2(MP2) values deviate from experiment by an average of 1.58 kcal mol^{-1}.[8]

To improve the accuracy of the method, isodesmic and isogeric reactions were used. Isodesmic reactions are those in which reactants and products contain the same type and same number of bonds. Isogeric reactions have equal numbers of unpaired electrons on both reactant and product sides of the reaction.[9] Because of the electronic similarity between reactants and products, errors in the calculated energy may cancel between them.

III. Results and Discussion

A. Structures of Fluorinated Ethers and Radicals. The structures of each ether and its corresponding radical are illustrated and tabulated in Figure 1 and Table 1, respectively. Dimethyl ether adopts a C_{2V} conformation with eclipsed methyl groups. The CO bond lengths in dimethyl ether are 1.414 Å. Two sets of hydrogen bonds exist, with the axial CH bonds (1.090 Å) being 0.009 Å longer than the equatorial CH bonds (1.099 Å). Atomic charge analysis at the MP2/6-31G(d) level of theory indicates that electron density is pulled toward the center of the molecule. The four equatorial hydrogens have atomic charges of 0.142, and the two axial hydrogens have atomic charges of 0.177. The difference in atomic charges between axial and equatorial hydrogens may influence which hydrogen in the ether is preferred for abstraction to generate the ether radical. The ether axial hydrogens have atomic charges

S1089-5639(98)01494-7 CCC: \$15.00

TABLE 1: Optimized Geometries[a] of Fluorinated Ether Radicals

	fluorinated ethers								fluorinated ether radicals							
	CH_3OCH_3		CH_3OCF_3		CHF_2OCHF_2		CF_3OCHF_2		CH_2OCH_3		CH_2OCF_3		CF_2OCHF_2		CF_2OCF_3	
coordinate	MP2	B3LYP	MP2	B3LYP	MP2	B3LYP	MP2	B3LYP	MP2	B3LYP	MP2	B3LYP	MP2	B3LYP	MP2	B3LYP
$R(C_3X_4)$	1.090	1.088	1.087	1.084	1.089	1.088	1.090	1.089	1.081	1.078	1.079	1.075	—	—	—	—
$R(C_3X_8)$	1.099	1.097	1.091	1.088	1.346	1.343	1.343	1.338	—	—	—	—	1.327	1.320	1.323	1.316
$R(C_3X_9)$	1.099	1.097	1.091	1.088	1.351	1.347	1.35	1.344	1.088	1.083	1.082	1.078	1.338	1.326	1.333	1.324
$R(C_2X_5)$	1.090	1.088	1.333	1.329	1.087	1.086	1.327	1.321	1.089	1.086	1.332	1.325	1.087	1.087	1.326	1.321
$R(C_2X_6)$	1.099	1.097	1.353	1.351	1.362	1.358	1.349	1.343	1.096	1.094	1.346	1.341	1.354	1.348	1.339	1.333
$R(C_2X_7)$	1.099	1.097	1.353	1.351	1.359	1.356	1.345	1.34	1.094	1.092	1.351	1.344	1.351	1.348	1.339	1.333
$R(C_2O)$	1.414	1.410	1.344	1.337	1.373	1.367	1.365	1.360	1.424	1.420	1.359	1.355	1.386	1.381	1.375	1.375
$R(C_3O)$	1.414	1.410	1.440	1.439	1.392	1.388	1.399	1.395	1.363	1.350	1.390	1.376	1.370	1.362	1.375	1.365
X_4C_3O	106.9	107.4	104.9	105.3	113.0	113.3	112.7	113.0	112.4	114.2	111.1	112.6	—	—	—	—
X_8C_3O	111.5	111.4	110.3	110.5	106.7	107.6	105.9	106.8	—	—	—	—	108.6	110.9	109.3	110.4
X_9C_3O	111.5	111.4	110.3	110.5	109.2	108.7	109.4	109.0	117.5	118.8	117.0	118.5	114.0	113.1	113.1	113.27
X_5C_2O	106.9	107.4	108.3	108.6	108.3	108.3	107.8	107.8	106.5	107.0	107.8	107.9	107.2	107.4	106.9	106.8
X_6C_2O	111.5	111.4	112.6	112.8	110.7	111.2	111.5	111.8	110.7	110.7	112.2	112.3	110.5	110.8	111.7	111.9
X_7C_2O	111.5	111.4	112.6	112.8	110.9	111.4	111.9	112.2	110.9	110.6	112.0	112.1	111.0	111.2	111.3	111.5
COC	111.1	112.9	114.4	116.4	114.9	117.7	115.2	117.6	113.5	115.6	115.5	117.8	116.4	117.7	115.0	117.4
$X_4C_3OC_2$	180.0	180.0	180.0	180.0	22.1	10.4	30.9	19.5	177.3	177.1	175.9	178.8	—	—	—	—
$X_8C_3OC_2$	−60.7	−60.7	−61.3	−61.3	143.4	132.0	151.9	140.9	—	—	—	—	173.1	135.26	150.9	141.4
$X_9C_3OC_2$	60.7	60.7	61.3	61.3	−100.1	−111.8	−91.3	−102.7	32.4	21.8	29.8	22.3	−62.6	100.3	−84.8	−93.8
$X_5C_2OC_3$	180.0	180.0	180.0	180.0	175.4	179.2	174.5	177.3	177.3	177.2	179.5	178.0	−167.8	177.5	−177.0	−178.2
$X_6C_2OC_3$	60.7	60.7	−60.1	−60.1	−63.9	−60.1	−65.8	−63.1	58.21	58.0	59.5	58.4	−47.3	−62.1	−57.2	−58.6
$X_7C_2OC_3$	−60.7	−60.7	60.1	60.1	53.9	58.1	54.1	57.1	−63.3	63.4	−60.9	−62.2	71.8	56.9	63.5	62.5

[a] Bond lengths in Angstroms and bond angles in degrees.

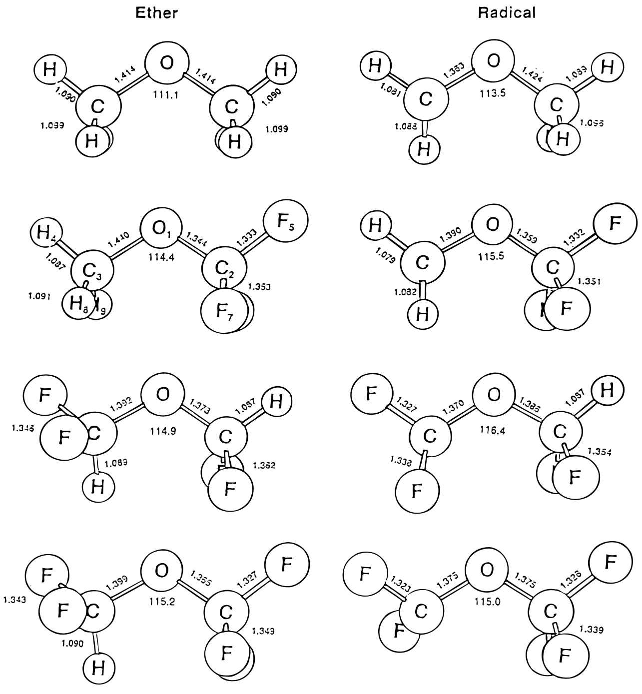

Figure 1. Structures of fluorinated ethers and related radicals optimized at the MP2(full)/6−31 g(d) level of theory: (a) CF_3OCH_3; (b) CHF_2-$OCHF_2$; (c) CF_3OCHF_2; (d) $CF_3OCH2^{\bullet}$; (e) $CHF_2OCF_2^{\bullet}$; (f) $CF_3OCF_2^{\bullet}$.

of 0.177, indicating that more of their electron density is removed than in the equatorial hydrogens, which have electron densities of only 0.142. The axial hydrogens, as mentioned, are also closer to the attached carbon atom (1.090 Å) than the equatorial hydrogens (1.099 Å). This result suggests a stronger bond between carbon and the axial hydrogens than between carbon and the equatorial hydrogens.

One of the two longer equatorial CH bonds of dimethyl ether is broken to form the ether radical. The corresponding dimethyl ether radical (CH_2OCH_3), shown in Table 1, displays C_1 symmetry with two CO bonds of differing length. The CO bond adjacent to the CH_2 group decreased in length relative to the parent ether from 1.414 to 1.363 Å, whereas the CO bond adjacent to the CH_3 group increased in length to 1.424 Å. All CH bonds decreased in length as the radical was formed. The most significant change involved the hydrogens on the CH_2 functional group of the radical. Originally 1.090 Å in dimethyl ether, the axial CH bond changed to 1.081 Å in length. This hydrogen retained a dihedral angle close to 180.0° (177.3°). The neighboring equatorial CH bond decreased in length from 1.099 to 1.088 Å. In addition, this hydrogen experienced a marked decrease in its dihedral angle, going from 60.7° in dimethyl ether to 32.4° in the radical.

CH_3OCF_3 adopts C_s symmetry, with eclipsed rather than staggered substituents. As expected, there is a marked change in the electron density distribution within the molecule as compared with dimethyl ether. Atomic charge analyses indicates that electron density is pulled toward the CF_3 functional group. The electron-withdrawing nature of the CF_3 group results in differing CO bond lengths in the ether. The CO bond adjacent to the CF_3 functional group decreases from 1.414 Å in dimethyl ether to 1.344 Å in E143a. Similarly, the opposing CO bond increases in length from 1.414 Å in dimethyl ether to 1.440 Å in E143a. Once again, the trend in axial versus equatorial atomic charges parallels the trend in CH bond length. The ether axial hydrogen has a partial positive charge of 0.208 and is 1.087 Å away from the attached carbon. The two ether equatorial hydrogens have partial positive charges of 0.195 and are located at a distance of 1.091 Å from the attached carbon atom. More electron density has been pulled from the axial hydrogen, which may translate into a shorter and stronger CH bond.

$^{\bullet}CH_2OCF_3$ has C_1 symmetry. As in $^{\bullet}CH_2OCH_3$, the CO bond adjacent to the CX_3 group has increased slightly from 1.344 Å in the parent ether to 1.359 Å in the radical, whereas the opposing CO bond has decreased in length from 1.440 to 1.390 Å. In contrast to $^{\bullet}CH_2OCH_3$, the CO bond adjacent to the CH_2 group is longer (1.390 Å) than the CO bond adjacent to the CF_3 group (1.359 Å) due to the electron-withdrawing nature of CF_3. The two remaining CH bond lengths decreased substantially. The axial C−H bond, originally 1.087 Å long decreased to 1.079 Å in the radical and has a dihedral angle of 176.0°, which is close to the original 180.0° for the parent ether. The

TABLE 2: Total Energies (in hartrees) for Species in Isodesmic Reactions

species	G2 (0K)	G2MP2 (0K)	G2 (298K)	G2MP2 (298K)
CH_3	−39.74373	−39.74254	−39.74058	−39.73940
CH_4	−40.40949	−40.40826	−40.40663	−40.40541
CH_3F	−139.55358	−139.54963	−139.55068	−139.54673
CH_2F_2	−238.71789	−238.71095	−238.71478	−238.70784
CHF_3	−337.89382	−337.88361	−337.89038	−337.88016
CF_4	−437.06677	−437.05315	−437.06286	−437.04924
HCO	−113.69890	−113.69603	−113.69604	−113.69317
CH_2O	−114.33905	−114.33619	−114.33621	−114.33335
CF_3OH	−413.05236	−413.03950	−413.04796	−413.03510
CH_3OCH_3	−154.74544	−154.74119	−154.74159	−154.73734
CH_3OCF_3	−452.26310	−452.24948	−452.25725	−452.24363
CHF_2OCHF_2	—	−551.40390	—	−551.39761
CF_3OCHF_2	—	−650.57182	—	−650.56494
·CH_2OCH_3	−154.09208	−154.08818	−154.08779	−154.08389
·CH_2OCF_3	−451.60212	−451.58846	−451.59634	−451.58268
·CF_2OCHF_2	—	−550.73559	—	−550.72930
·CF_2OCF_3	—	−649.90436	—	−649.89746

TABLE 3: Known Thermodynamic Constants for Species involved in Isodesmic Reactions[a]

species	$\Delta H_{f,0K}$	$\Delta H_{f,298K}$	bond dissociation energy (BDE)	reference
H_2O	−57.10 ± 0.01	−57.80 ± 0.01	119.3 ± 1.0	*h, f*
OH	9.3 ± 0.1	9.4 ± 0.1	—	*h*
CH_4	−16.0 ± 0.1	−17.9 ± 0.1	104.3 ± 0.2	*h, f*
CH_3	35.8 ± 0.1	35.0 ± 0.1	—	*h*
CH_3F	−55.5 ± 1.2	−57.4 ± 1.2	—	*g*
CH_2F_2	−105.9 ± 0.4	−107.7 ± 0.4	—	*b*
CHF_3	−164.9 ± 0.8	−166.6 ± 0.8	—	*b*
CF_4	−221.6 ± 0.3	−223.0 ± 0.3	—	*b*
CH_2O	−25.1 ± 0.1	−26.0 ± 0.1	88.3 ± 1.0	*h*
HCO	9.9 ± 0.2	10.0 ± 0.2	—	*h*
CF_3OH	−215.5 ± 2.0	−217.7 ± 2.0	—	*c, d*
CH_3OH	−45.4 ± 0.1	−48.0 ± 0.1	—	*h*
CH_3OCH_3	−39.7 ± 0.1	−44 ± 0.1	95.5	*e, f*
CH_2OCH_3	4.2	0.9		*e, f*

[a] All values in kcal mol^{-1}. [b] Chase, M. W.; Davies, C. A.; Downey, J. R.; Frurip, D. J.; McDonald, R. A.; Syverud, A. N. *J. Phys. Chem. Ref. Data* **1985**, *14*, (Supplement 1). [c] Montgomery, J. A.; Michels, H. H.; Francisco, J. S. *Chem. Phys. Lett.* **1994**, *220*, 391. [d] Lias, S. G.; Bartmess, J. E.; Liebman, J. F.; Holmes, J. L.; Levin, R. D.; Mallard, W. G. *J. Phys. Chem. Ref. Data*, **1988**, *17*, (Supplement 1). [e] Good, D. A.; Francisco, J. S. *J. Chem. Phys. Lett.* **1997**, *266*, 512. [f] Griller, D.; Kanabus-Kaminska, J. M.; Maccol, A. THEOCHEM **1988**, *163*, 125. [g] Espinosa-Garcia, J. *J. Chem. Phys. Lett.* **1996**, *250*, 71. [h] Curtiss, L. A.; Raghavachari, K.; Redfern, P. C.; Pople, J. A. *J. Chem. Phys.* **1997**, *106(3)*, 1063.

equatorial hydrogen also decreased from 1.091 to 1.082 Å. As in $^{\bullet}CH_2OCH_3$, this dihedral angle decreased significantly from 61.3° to 29.8°. In addition, the COC angle has increased from 114.4° in CH_3OCF_3 to 115.5° in CH_3OCF_2. The fluorine atoms remain virtually unchanged in going from parent ether to ether radical.

CHF_2OCHF_2 exists in C_1 symmetry with both hydrogens in axial postitions arranged anti with respect to each other. Unlike the previous two ethers, E134 contains no equatorial hydrogens. The upwardly oriented hydrogen has a positive atomic charge of 0.208, whereas the downwardly oriented hydrogen has a positive atomic charge of 0.193. Once again, the hydrogen atom with the most electron density has a longer CH bond and is preferred for abstraction. The upwardly oriented hydrogen has a shorter bond length of 1.087 Å compared with the 1.089 Å CH bond length of the downwardly oriented hydrogen. The CH bond oriented downward in CHF_2OCHF_2 breaks to form the ether radical $^{\bullet}CF_2OCHF_2$.

The remaining CH bond in the radical is outwardly oriented with a length identical to that found in the parent ether. The two CF bonds on that side of the ether decrease slightly whereas the two opposing CF bonds decrease in length going from the ether to the radical (F_1:1.346 Å → 1.327 Å; F_2: 1.351 Å → 1.338 Å). As with the previous two ethers, the CO bond adjacent to the hydrogen increases in length from 1.373 Å in the ether to 1.386 Å in the ether radical. The opposing CO bond decreases in length from 1.392 Å in the ether to 1.369 Å in the ether radical. The COC angle also increases from 114.9° to 116.4° in the radical.

CF_3OCHF_2 also exists in C_1 symmetry. Its sole CH bond is oriented underneath the molecule with a slightly larger CH bond (1.090 Å) than the ones found in CHF_2OCHF_2 (1.089 and 1.087 Å). The two CO bonds in CF_3OCHF_2 also equilibrate when forming the radical; one increases in length from 1.365 to 1.375 Å, whereas the other CO bond decreases in length from 1.399 to 1.375 Å. The COC angle remains fairly constant at 115.0°. As the CH bond in the ether breaks, all CF bonds decrease in length slightly.

B. Thermochemistry of Fluorinated Ethers and Radicals. Table 2 tabulates the energies computed at 0 and 298 K for each species using both G2 and G2(MP2) methodology. The total energies are corrected to 0 K by adding the zero-point energy to the predicted total energy. To obtain the energy at 298 K, the thermal energy of each species is added to its total energy instead of the zero-point energy. The reaction enthalpy at 0 K or 298 K is then obtained by use of the corrected energy along with eq 1:

$$\Delta H = \Delta E - \Delta nRT \tag{1}$$

For a reaction with the same number of products as reactants, the change in molecularity, Δn, is zero and $\Delta H = \Delta E$. The enthalpy of formation of a species is determined by subtracting the known heats of formation of the other species involved in the reaction from the reaction enthalpy. Table 3 lists thermodynamic properties for all species used in isodesmic reactions.[10−16] Table 4 lists heats of formation for each ether and the corresponding ether radical computed from the aforementioned methodology. The isodesmic reactions in Table 4a involve methane and its fluorinated derivatives. Each fluorinated ether is defluorinated through the exchange of CF bonds in the ether for CH bonds from methane and its derivatives. Each of the species used is a stable, closed-shell species.

The heat of formation of dimethyl ether was calculated for calibration purposes using reaction 2:

$$CH_3OCH_3 + H_2O \rightarrow CH_3OH + CH_3OH \tag{2}$$

The heat of formation of CH_3OCH_3 was determined to be −39.9 kcal mol^{-1} at 0 K and −44.1 kcal mol^{-1} at 298 K by the G2(MP2) theory. Using G2 theory, values of −39.7 and −43.9 kcal mol^{-1} were obtained. Values using both theories are in excellent agreement with the literature values of −39.7 and −44.0 kcal mol^{-1} at 0 and 298 K, respectively.[12]

The substitution of three hydrogens with three fluorines to form E143a has a pronounced effect on the heat of formation. G2 theory predicts the heats of formation of E143a to be −209.3 and −212.7 kcal mol^{-1} at 0 and 298 K, respectively. G2(MP2) theory finds the heats of formation to be −209.2 and −212.7 kcal mol^{-1} at 0 and 298 K, respectively. As shown by these values, there is virtually no difference in the heats of formation predicted by the G2 and G2(MP2) levels of theory. Thus, for the remaining two ethers, only the G2(MP2) values were

TABLE 4: Heats of Formation (kcal mol^{-1}) of Fluorinated Ethers and Fluorinated Ether Radicals[a]

compound	Isodesmic Scheme	ΔH_f (0 K)	ΔH_f (298 K)
	(a) fluorinated ethers		
CH_3OCF_3	$CF_3OCH_3 + H_2O \rightarrow CF_3OH + CH_3OH$	−209.4 + 2.9	−212.8 ± 2.9
	$CF_3OCH_3 + CH_2F_2 + CF_3H \rightarrow CH_3OCH_3 + CF_4 + CF_4$	−209.7 ± 1.8	−213.1 ± 1.8
	$CF_3OCH_3 + CH_4 \rightarrow CH_3OCH_3 + CHF_3$	−209.0 ± 2.0	−212.5 ± 2.0
	$CF_3OCH_3 + CH_3F \rightarrow CH_3OCH_3 + CF_4$	−208.5 ± 2.4	−212.0 ± 2.4
		−209.2 ± 2.3	−212.7 ± 2.3
CHF_2OCHF_2	$CHF_2OCHF_2 + CH_3F + CH_3F \rightarrow CH_3OCH_3 + CHF_3 + CHF_3$	−255.0 ± 1.9	−258.3 ± 1.9
	$CHF_2OCHF_2 + CH_4 \rightarrow CH_3OCH_3 + CF_4$	−256.2 ± 2.3	−259.4 ± 2.3
	$CHF_2OCHF_2 + CH_4 + CH_3F \rightarrow CH_3OCH_3 + CHF_3 + CH_2F_2$	−255.1 ± 1.8	−258.3 ± 1.8
	$CHF_2OCHF_2 + CH_2F_2 + CH_2F_2 \rightarrow CH_3OCH_3 + CF_4 + CF_4$	−257.2 ± 1.7	−260.5 ± 1.7
		−255.9 ± 1.9	−259.1 ± 1.9
CF_3OCHF_2	$CF_3OCHF_2 + CH_4 + CH_2F_2 \rightarrow CH_3OCH_3 + CHF_3 + CF_4$	−312.3 ± 1.8	−315.2 ± 1.8
	$CF_3OCHF_2 + CH_4 + CH_3F \rightarrow CH_3OCH_3 + CH_2F_2 + CF_4$	−310.8 ± 1.8	−313.7 ± 1.8
	$CF_3OCHF_2 + CH_2F_2 + CH_3F \rightarrow CH_3OCH_3 + CF_4 + CF_4$	−311.3 ± 1.8	−314.2 ± 1.8
	$CF_3OCHF_2 + CH_4 + CH_4 \rightarrow CH_3OCH_3 + CF_3H + CH_2F_2$	−311.8 ± 1.7	−314.7 ± 1.7
		−311.5 ± 1.8	−314.5 ± 1.8
	(b) fluorinated ether radicals		
CH_2OCF_3	$CF_3OCH_3 + CH_3 \rightarrow CH_4 + CF_3OCH_2$	−160.4 ± 2.7	−163.0 ± 2.7
	$CF_3OCH_3 + HCO \rightarrow CH_2O + CF_3OCH_2$	−161.1 ± 2.7	−163.7 ± 2.7
	$CF_3OCH_3 + CH_3OCH_2 \rightarrow CH_3OCH_3 + CF_3OCH_2$	−160.5 + 2.7	−163.1 + 2.7
	$CF_3OCH_2 + CH_4 + CH_4 \rightarrow CHF_3 + CH_3 + CH_3OCH_3$	−160.2 ± 2.0	−162.8 ± 2.0
		−160.6 ± 2.5	−163.2 ± 2.5
CHF_2OCF_2	$CHF_2OCHF_2 + CH_3 \rightarrow CH_4 + CHF_2OCF_2$	−202.5 ± 2.6	−204.8 ± 2.6
	$CHF_2OCHF_2 + HCO \rightarrow CH_2O + CHF_2OCF_2$	−203.3 ± 2.6	−205.4 ± 2.6
	$CHF_2OCHF_2 + CH_3OCH_2 \rightarrow CH_3OCH_3 + CHF_2OCF_2$	−202.7 + 2.6	−204.9 + 2.6
	$CHF_2OCF_2 + CH_4 + CH_4 \rightarrow CF_4 + CH_3 + CH_3OCH_3$	−202.8 ± 1.9	−205.1 ± 1.9
		−202.8 ± 2.4	−205.1 ± 2.4
CF_3OCF_2	$CF_3OCHF_2 + CH_3 \rightarrow CH_4 + CF_3OCF_2$	−258.7 ± 2.6	−260.6 ± 2.6
	$CF_3OCHF_2 + HCO \rightarrow CH_2O + CF_3OCF_2$	−259.4 ± 2.6	−261.3 ± 2.6
	$CF_3OCHF_2 + CH3OCH_2 \rightarrow CH_3OCH_3 + CF_3OCF_2$	−258.8 + 2.6	−260.7 + 2.6
	$CF_3OCF_2 + CH_4 + CH_4 + CH_4 \rightarrow C\ F_4 + CH_3 + CH_3F + CH_3OCH_3$	−259.5 ± 1.5	−261.4 ± 1.5
		−259.1 ± 2.3	−261.0 ± 2.3

[a] All values derived from G2(MP2) energies.

determined, as they are computationally less expensive. The values in Table 4 were derived from G2(MP2) energies. The substitution by a fourth fluorine atom to form E134 results in an additional 46.7 kcal mol^{-1} increase in stability, whereas substitution by a fifth fluorine atom forming E125 results in an additional 55.6 kcal mol^{-1} increase.

The first three isodesmic reactions in Table 4b were used to calculate the ether radical heat of formation, by using the heat of formation of the parent ether listed in Table 4a. Unlike the first three isodesmic schemes in the reaction set, which involve CH bond cleavage in the parent ether to form the radical, the fourth isodesmic reaction involves only the radical and is not dependent on the properties of the parent ether. The results of the fourth isodesmic are consistent with the first three isodesmic schemes. As in the case of the parent ethers, the heats of formation of the radicals decrease with increasing fluorination.

The total error associated with each determination is a function of the uncertainty in the G2(MP2) energies and the uncertainty in the heats of formation of the species in Table 3. Curtiss et al.[16] found an average absolute deviation from experiment of 3.5 kcal mol^{-1} for species containing multiple fluorine atoms at the G2(MP2) level of theory. Thus, 3.5 kcal mol^{-1} was used in this investigation as a reasonable estimate of the error associated with G2(MP2) energy calculations. For the parent ether, the uncertainty in the heat of formation at both 0 and 298 K is ±2.0 kcal mol^{-1}, or ∼1.0%. As shown in Table 4b, the uncertainty in the heats of formation of the ether radicals in the first three isodesmic schemes of the reaction set is higher than the uncertainty in the heats of formation of the parent ethers. This result is due to the fact that the first three isodesmic schemes of the set include the 2.0 kcal mol^{-1} uncertainty from the parent ether. The uncertainty in the heats of formation for the ether radicals in the fourth isodesmic scheme of each reaction set is again under ±2.0 kcal mol^{-1}. This result is due to the fact that these reactions are independent of the parent ether and the error associated with it.

C. CH Bond Dissociation Energies for the Fluorinated Ethers. Section A examined the functional group differences and the resulting structural differences of each ether. An important consequence of these substituent effects is a change in the CH bond dissociation energy, which in turn influences the activation energies and rate constants for hydrogen abstraction reactions. Hsu et al.[3] employed a relative rate technique to measure temperature-dependent rate constants for each of the fluorinated ethers with hydroxyl radical. The relative rate technique measured the rate constants relative to species such as CH_4, CH_3CCl_3, HFC-152A, HFC-32, and HFC-125. Absolute rate constants were then extracted for each ether using known OH reaction rate constants for the aforementioned reference gases.[3] The relative rate technique negates the effects of unwanted side reactions caused from impurities. As a result, the rate data from Hsu et al.'s investigation[3] are substantially slower than previous determinations. Hsu et al.[3] notes a correlation between the log of the normalized rate constant and the CH bond dissociation energy [i.e., $\log(k(298\text{ K})/n(\mathrm{H}))$, where k is the rate constant at 298 K and n(H) is the number of hydrogens within the parent molecule]. Using this correlation, Hsu et al.[3] inferred values for the CH bond energies of the ethers.

TABLE 5: CH Bond Dissociation Energies (kcal mol^{-1}) for Fluorinated Ethers

species	G2(MP2) using isodesmic reactions	using heats of formation from Table 4	average columns 2 and 3	B3LYP/ 6-311++G(3df,3pd)	experiment
CH_3OCH_3	96.4 ± 2.4	97.0[c]	96.7 ± 2.4	94.8	95.5[a]
CH_3OCF_3	101.1 ± 2.8	101.6 ± 2.4	101.4 ± 2.6	100.2	102 ± 1.0[b]
CHF_2OCHF_2	105.7 ± 2.7	106.1 ± 2.1	105.9 ± 2.4	103.4	104 ± 1.0[b]
CF_3OCHF_2	105.3 ± 2.7	105.6 ± 2.1	105.5 ± 2.4	103.5	106 ± 1.0[b]

[a] Louks, L. F.; Larden, K. J. *Can. J. Chem.* **1967**, *45*, 2763. [b] Hsu, K. J.; DeMore, W. B. *J. Phys. Chem.* **1995**, *99*, 11141. [c] Good, D. A.; Francisco, J. S. *Chem. Phys. Lett.* **1997**, *266*, 512.

TABLE 6: Enthalpies of Reaction (kcal mol^{-1}) Between Hydroxyl Radical and Ether at 298 K

species	heats of reaction[a] from heats of formation	heats of reaction[b] from bond dissociation energies	heats of reaction[c] from bond dissociation energies
CH_3OCH_3	−22.3	−22.6	−23.8
CH_3OCF_3	−17.7	−17.9	−17.3
CHF_2OCHF_2	−13.2	−13.4	−15.3
CF_3OCHF_2	−13.7	−13.8	−13.3

[a] Using heats of formation from Tables 3 and 4. [b] Using BDEs from present work. [c] Using BDEs from Hsu et al.[3]

There exists an uncertainty of 1 kcal mol^{-1} in the fit aside from uncertainties in the bond dissociation energies of the species used to generate the fit. Our present work also determines the CH bond dissociation energies of these ethers, thus allowing us to comment on the rate data of Hsu et al.[3]

The isodesmic schemes used to calculate the heats of formation for each ether radical are also used to calculate the CH bond strengths of the parent ether. For instance, the enthalpy of reaction between methyl radical and E143a (reaction 3) is equal to

$$CH_3OCF_3 + CH_3 \rightarrow CH_4 + CH_2OCF_3 \tag{3}$$

the difference in CH bond strengths between methane and CH_3OCF_3. Table 5 (column 2) lists the bond dissociation energy for each ether calculated in this manner.

The error associated with this determination is composed of two factors. The first is the error in determining the enthalpy of reaction from G2(MP2) energies, which for each ether is 3.50 kcal mol^{-1}. The second factor is the uncertainty in the bond dissociation energy of the opposing product, which, in this illustration, is CH_4 (±0.2 kcal mol^{-1} from Table 3). Thus, after averaging the values from the first three isodesmic schemes in Table 4b, each ether in Table 5 (column 2) has an uncertainty on the order of 2.7 kcal mol^{-1}.

Table 5 (column 3) shows the bond dissociation energy of each ether using the fact that the BDE is the enthalpy of the dissociation reaction, that is

$$CH_3OCF_3 \rightarrow CH_2OCF_3 + H^{\bullet} \tag{4}$$

To perform the calculation, the heat of formation of each ether species was taken from Table 4 and the hydrogen radical heat of formation was taken as 52.1 kcal mol^{-1} at 298 K. The error associated with this determination was determined from the errors of the individual heats of formation of each species. Column 4 of Table 5 uses columns 2 and 3 to tabulate an average CH bond dissociation energy for each ether.

Dimethyl ether was found to have an average CH bond strength of 96.7 ± 2.4 kcal mol^{-1}, which is well within the literature value of 95.5 kcal mol^{-1}.[14] The equatorial hydrogens on CH_3OCF_3 (E143a) have a CH bond strength of 101.4 kcal mol^{-1}. The increase in CH bond strength between dimethyl ether and E143a can be rationalized through inspection of their respective structures. As shown in Table 1, the CH bonds in E143a are, on average, 0.007 Å shorter than those in dimethyl ether. Shorter bond lengths in E143a translate into higher bond dissociation energies and ultimately into slower reaction rates with the hydroxyl radical. The CH bond strength of E143a was determined to be 101.4 ± 2.6 kcal mol^{-1}, which is within the experimental value of 102 ± 1.0 kcal mol^{-1}.

The substitution by another fluorine to form CHF_2OCHF_2 results in an additional increase in the CH bond strength to 105.9 ± 2.4 kcal mol^{-1}, which is within the experimental value of 104.0 ± 1.0 kcal mol^{-1}. For CF_3OCHF_2, the CH bond strength was predicted to be 105.5 kcal mol^{-1}, which is 0.4 kcal mol^{-1} in energy lower than the CH bond strength of CHF_2OCHF_2. When considering the error associated with the determination, the CH bond strengths of E125 and E134 are indistinguishable. The CH bond lengths in E134 and E125 are also indistinguishable. As shown in Table 1, the CH distance in E125 is 1.090 Å, whereas the hydrogen removed in E134 has a length of 1.089 Å.

To further verify the trend in bond dissociation energies, the ethers and their radicals were optimized at the B3LYP level of theory with the large 6-311++G(3df,3pd) basis set. The CH bond-breaking isodesmic schemes, presented in Table 4b, are once again used for the determination. The results are presented in Table 5 (column 5) with experimental values from Hsu et al.[3] in column 6.[3,13,17] The B3LYP values are lower than the G2(MP2) values, but the same trends exist. The bond dissociation energies for E134 and E125 are once again indistinguishable, differing by only 0.1 kcal mol^{-1}.

The CH bond strengths determined in this study are within the experimental error of those determined in the work of Hsu et al.[3] and lend support to the results determined in that investigation.

Table 6 summarizes the enthalpy of reaction at 298 K for each ether with the hydroxyl radical to form water and an ether radical. The enthalpies were calculated by several different ways. The values in column 2 were calculated using the determined heats of formation of the ether and radical (Table 4) along with the known heats of formation for water and OH (Table 3). Columns 3 and 4 used the fact that the enthalpy of this reaction is equal to the difference between the O—H bond strength in water and the C—H bond strength of the ether. The OH bond strength of water is given in Table 3 as 119.3 ± 1.0 kcal mol^{-1}. Column 3 used the bond dissociation energies of each ether as computed in the present work, whereas those in column 4 were derived from the bond dissociation energies of Hsu et al.[3] The different methods used in Table 6 yield similar results, suggesting that the results shown in this work are consistent and within the error limits of the experimental determinations. Moreover, this similarity lends support to our determinations of the heats of formation of the ethers and their radicals.

IV. Conclusion

Dimethyl ether is the least stable of the ethers, with a heat of formation of −44.0 kcal mol^{-1}. It has four equivalent equatorial hydrogens and a CH bond dissociation energy of 96.7 kcal mol^{-1}. Its reaction with the hydroxyl radical is exothermic by −22.5 kcal mol^{-1}, producing water and the ether radical $^{\bullet}CH_2$-OCH_3.

The substitution by three fluorine atoms results in increased stability compared with dimethyl ether. E143a has a heat of formation of −212.7 kcal mol^{-1}. Its two equivalent equatorial hydrogens have a bond dissociation energy of 101.4 kcal mol^{-1}. Its reaction with OH is exothermic by −17.8 kcal mol^{-1}. The formed ether radical has a heat of formation of −163.2 kcal mol^{-1}.

E134 has two axial hydrogens, the longer of which (1.089 Å) is abstracted to form the radical. Breaking this bond requires 105.9 kcal mol^{-1}. The stability at 298 K of E134 and its radical are −259.1 and −205.1 kcal mol^{-1}, respectively. Its reaction with the hydroxyl radical is exothermic by −13.3 kcal mol^{-1}.

E125 is very stable, with a heat of formation of −314.5 kcal mol^{-1}. Its sole hydrogen is oriented toward the inside of the molecule in a rather shielded environment. To break this CH bond requires 105.5 kcal mol^{-1}. The formed ether radical has a heat of formation of −261.0 kcal mol^{-1}. The reaction with hydroxyl radical is exothermic by −13.8 kcal mol^{-1}. E125 and E134 have many identical properties. Their CH bond lengths (1.090 versus 1.089 Å), CH bond strengths (105.5 versus 105.9 kcal mol^{-1}), and reaction enthalpies with OH (−13.8 versus −13.3 kcal mol^{-1}) are virtually indistinguishable.

Acknowledgment. We thank the computer center at JPL for ample provision of computing resources that made this work possible. Funding from the NASA Office of Mission to Planet Earth, Aeronautics and Space Science provided the Cray supercomputer used in the investigation.

References and Notes

(1) Zhang, Z.; Saini, R. D.; Kurylo, M. J. *J. Phys. Chem*. **1992**, *96*, 9301.

(2) Cooper, D. L.; Cunningham, T. P.; Allan, N. L.; McCulloch, A. *Atmos. Environ*. **1992**, *26*, 1331.

(3) Hsu, K. J.; DeMore, W. B. *J. Phys. Chem.* **1995**, *99*, 11141.

(4) Gaussian 94 Revision D.2: Frisch, M. J.; Trucks, G. W.; Schlegel, H. B.; Gill, P. M. W.; Johnson, B. G.; Robb, M. A.; Cheeseman, J. R.; Keith, T.; Peterson, G. A.; Montgomery, J. A.; Raghavachari, K.; Al-Laham, M. A.; Zakrzewski, V. G.; Ortiz, J. V.; Foresman, J. B.; Cioslowski, J.; Stefanov, B. B.; Nanayakkara, A.; Challacombe, M.; Peng, C. Y.; Ayala, P. Y.; Chen, W.; Wong, M. W.; Andres, J. L.; Replogle, E. S.; Gomperts, R.; Martin, R. L.; Fox, D. J.; Binkley, J. S.; DeFrees, D. J.; Baker, J.; Stewart, J. P.; Head-Gordon, M.; Gonzalez, C.; Pople, J. A. Gaussian, Inc. Pittsburgh, PA, 1995.

(5) Lee, C.; Yang, W.; Parr, R. G. *Phys. Rev. B* **1988**, *41*, 785.

(6) Curtiss, L. A.; Raghavachari, K.; Trucks, G. W.; Pople, J. A. *J. Chem. Phys*. **1991**, *94*, 7221.

(7) Pople, J. A.; Head-Gordon, M.; Fox, D. J.; Raghavachari, K.; Curtiss, L. A. *J. Chem. Phys*. **1989**, *90*, 5622.

(8) Curtiss, L. A.; Raghavachari, K.; Pople, J. A. *J. Chem. Phys*. **1993**, *98*, 1293.

(9) Hehre, W. J.; Radom, L.; Schleyer, P. von R.; Pople, J. A. *Ab Initio Molecular Orbital Theory*; Wiley: New York, 1986.

(10) Chase, M. W.; Davies, C. A.; Downey, J. R.; Frurip, D. J.; McDonald, R. A.; Syverud, A. N. *J. Phys. Chem. Ref. Data* **1985**, *14*, Supplement 1.

(11) Montgomery, J. A.; Michels, H. H.; Francisco, J. S. *Chem. Phys. Lett*. **1994**, *220*, 391.

(12) Lias, S. G.; Bartmess, J. E.; Liebman, J. F.; Holmes, J. L.; Levin, R. D.; Mallard, W. G. *J. Phys. Chem. Ref. Data* **1988**, *17*, Supplement 1.

(13) Good, D. A., Francisco, J. S. *Chem. Phys. Lett*. **1997**, *266*, 512.

(14) Griller, D.; Kanabus-Kaminska, J. M.; Maccol, A. *Theochem*. **1988**, *163*, 125.

(15) Espinosa-Garcia, J. *Chem. Phys. Lett*. **1996**, *250*, 71.

(16) Curtiss, L. A., Raghavachari, K., Redfern, P. C., Pople, J. A. *J. Chem. Phys*. **1997**, *106*(*3*), 1063.

(17) Louks, L. F.; Larden, K. J. *Can. J. Chem*. **1967**, *45*, 2763.